$[k_{obsd}/((porphyrin)Fe^{III}Cl)]$ for reaction with NO are in the order $(Me_8TPP)Fe^{III}Cl:(TPP)Fe^{III}Cl:(Cl_8TPP)Fe^{III}Cl = 1:3:235$. There are two conclusions to be drawn: (i) the more electron deficient the iron(III) porphyrin moiety is the greater the rate constant for oxygen transfer from NO to the ligated iron(III) is and (ii) demethylation of *N,N*-dimethyl- and *N*-methylanilines is more sensitive to the electronic nature of the iron(IV)–oxo porphyrin π-cation radical than is epoxidation, though the rate constants for both processes must increase with a decrease in the electron density of the higher valent iron–oxo species.

Conclusion. The immediate products of the reaction of $(Me_8TPP)Fe^{III}Cl$ with NO are DA and a higher valent iron–oxo porphyrin which, on the basis of other studies,[2] can be assigned the structure of an iron(IV)–oxo porphyrin π-cation radical ($(^{+\bullet}Me_8TPP)Fe^{IV}O$). Reaction of 1 and 2 equiv of the latter with DA provides MA and FA, respectively, and its further involvement in the oxidation of MA yields MD, H, and A. Under the pseudo-first-order conditions of $[NO]_i \gg [(Me_8TPP)Fe^{III}Cl]_i$ each of the products DA, MA, FA, MD, H, and A appear with the same pseudo-first-order rate constant. Two inevitable conclusions can be reached: (i) ligation of NO to the catalyst $(Me_8TPP)Fe^{III}Cl$ does not involve saturation of the latter, and (ii) the rate-determining step involves oxygen transfer from N → iron(III) within the $Me_8TPP(Cl)Fe^{III}ON$ complex to provide DA and the higher valent iron–oxo porphyrin. Epoxidation yields with six alkenes (at 1.0 M) range between 100% and 80% (based upon the initial concentration of NO) when using $(Me_8TPP)Fe^{III}Cl$ as catalyst. The epoxidations are not rate-controlling. The use of NO with $(Me_8TPP)Fe^{III}Cl$ provides a very mild method for alkene epoxidation in high yields. By use of the sterically hindered $(Me_8TPP)Fe^{III}Cl$ there is prevented the reaction of $[(Me_8TPP)Fe^{III}]^+$ with $(^{+\bullet}Me_8TPP)Fe^{IV}O$ to yield $[(Me_8TPP)Fe^{IV}]_2O$. Complications of kinetic interpretations by such a reaction have been considered by Nolte and associates.[12]

Acknowledgment. This work was supported by grants from the National Institutes of Health and the National Science Foundation.

(12) Nolte, R. J. M.; Razenberg, J. A. S. J.; Schurman, R. *J. Am. Chem. Soc.* **1986**, *108*, 2751.

Dimerization Energetics of Benzene and Aromatic Amino Acid Side Chains

S. K. Burley*[†,§] and G. A. Petsko[†]

Contribution from the Department of Chemistry Massachusetts Institute of Technology, Cambridge, Massachusetts 02139, and Harvard Medical School, Health Sciences and Technology Division, Boston, Massachusetts 02115. *Received April 22, 1986*

Abstract: Interactions between aromatic side chains in protein crystal structures have been studied by geometric analysis and nonbonded interaction energy calculations, based on ab initio quantum mechanical calculations of dibenzene. Aromatic side chains in proteins pair with preferred centroid separations of between 3.4 and 6.5 Å. Eighty-four percent of these aromatic pairs make enthalpically favorable edge-to-face interactions, which bring a $\delta(+)$ hydrogen atom of one aromatic ring near to the $\delta(-)$ π-electron cloud of the other aromatic ring. The distribution of observed interaction geometries differs substantially from random and depends critically on the spatial arrangement of the two aromatic rings. These data demonstrate that the edge-to-face interaction of two aromatic side chains makes an enthalpic contribution of between −1 and −2 kcal/mol to the energy stabilization of a protein and does not arise solely as a function of packing constraints.

Recent surveys of aromatic side chain environments in single-crystal peptide structures and in protein crystal structures have documented statistically preferred interaction geometries between aromatic rings and neighboring atoms such as carbonyl oxygens, sulfurs, and amino groups.[1-4] In addition, Thomas et al.[2] used ab initio calculations to demonstrate that an enthalpically favorable interaction between the $\delta(+)$ hydrogen atoms of aromatic side chains and the $\delta(-)$ carbonyl oxygen atoms is responsible for their preferred interaction geometry, observed in protein and peptide crystal structures.

Edge-to-face packing of crystalline aromatic compounds was first appreciated in single-crystal structures of benzene[5] and its derivatives.[6] Such arrangements bring a $\delta(+)$ hydrogen atom of one aromatic group into close contact with the $\delta(-)$ π-electron cloud of the other aromatic ring and are energetically favorable.[7,8] Similar arrangements of aromatic groups have been detected in surveys of aromatic side-chain environments of proteins by Burley and Petsko[9] and Singh and Thornton.[10] The present investigation extends these analyses by using the results of ab initio calculations of benzene dimerization to further characterize interactions between pairs of neighboring aromatic side chains in protein crystal structures.

Procedures

Geometric Analysis. Thirty-three high-resolution (<2 Å), refined protein crystal structures were examined for aromatic side chains near one another. Their packing geometry was analyzed with use of a right-handed polar coordinate system, which places the center of mass of one of the two six-membered rings, the reference ring, at the origin. Its 6-fold symmetry axis is colinear with the z axis, and the C_β–C_γ bond

* Author to whom correspondence should be addressed.
† Massachusetts Institute of Technology.
§ Harvard Medical School.

(1) Gould, R. O.; Gray, A. M.; Taylor, P.; Walkinshaw, M. D. *J. Am. Chem. Soc.* **1985**, *107*, 5921.
(2) Thomas, K. A.; Smith, G. M.; Thomas, T. M.; Feldman, R. J. *Proc. Natl. Acad. Sci. U.S.A.* **1982**, *79*, 4843.
(3) Reid, K. S. C.; Lindley, P. F.; Thornton, J. M. *FEBS Lett.* **1985**, *190*, 209.
(4) Burley, S. K.; Petsko, G. A. P. *FEBS Lett.* **1986**, *203*, 139.
(5) Cox, E. G.; Cruickshank, D. W. J.; Smith, J. A. S. *Proc. R. Soc. London* **1958**, *247*, 1.
(6) Wyckoff, R. W. G. *Crystal Structures, The Structure of Benzene Derivatives*; Interscience: New York, 1969, Vol. 6.
(7) Karlström, G.; Linse, P.; Wallqvist, A.; Jonsson, B. *J. Am. Chem. Soc.* **1983**, *105*, 3777.
(8) Pawliszyn, J.; Szczesniak, M. M.; Scheiner, S. *J. Phys. Chem.* **1984**, *88*, 1726.
(9) Burley, S. K.; Petsko, G. A. *Science* **1985**, *229*, 23.
(10) Singh, J.; Thornton, J. M. *FEBS Lett.* **1985**, *191*, 1.
(11) Steed, J. M.; Dixon, T. A.; Klemperer, W. J. *J. Chem. Phys.* **1979**, *70*, 4940.

0002-7863/86/1508-7995$01.50/0

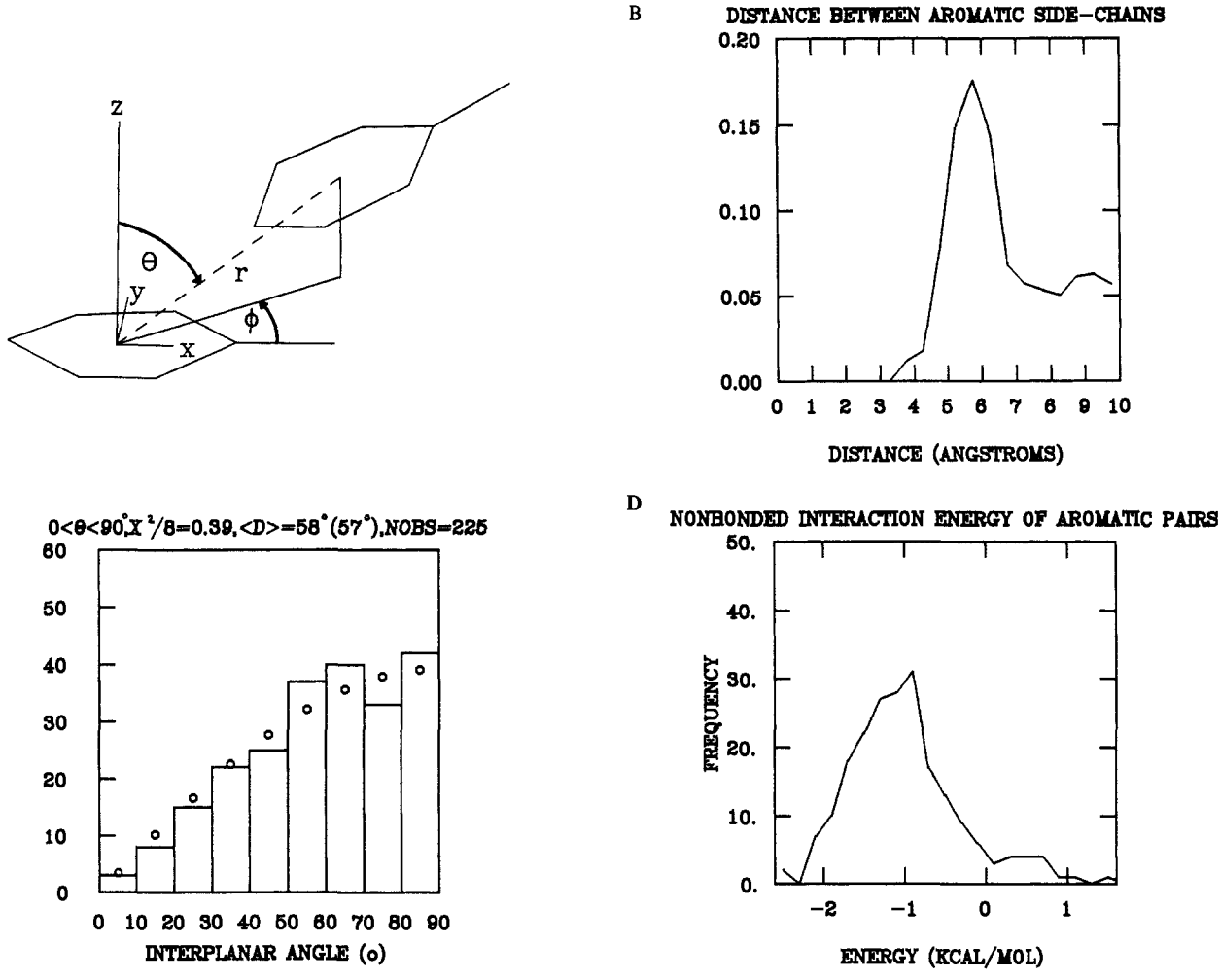

Figure 1. (A) Coordinate axes for the reference aromatic side chain, and the definition of the polar coordinate system (r, θ, ϕ). Thirty-three coordinate datasets were used in analysis of proteins: actinidin (P2ACT), avian pancreatic polypeptide (P1PPT), carbonic anhydrase C(P1CAC), carboxypeptidase A(P1CPA), concanavalin A (P2CNA), crambin (P1CRN), cytochrome b_5 (P2B5C), cytochrome c (P4CYT), cytochrome c_{551} (P251C), erythrocrourin (P1ECD), immunoglobulin-FAB fragment (P3FAB), ferredoxin (P1FDX,P2FD1), flavodoxin (P4FXN), hemoglobin (P1LHB), hemoglobin α-chain (P2MHB), hemoglobin β-chain (P2MHB), high potential iron protein (P1HIP), insulin (P1INS), lactate dehydrogenase (P4LDH), leghemoglobin (P1HBL), lysozyme (P2LYZ), myoglobin,[20] neurotoxin,[21] parvalbumin (P3CPV), phospholipase A_2 (P1BP2), plastocyanin (P1PCY), prealbumin (P2PAB), pancreatic trypsin inhibitor (P3PTI), Bence-Jones REI protein (P1REI), ribonuclease A,[22] superoxide dismutase (P2SOD), and trypsin (P1PTN). The abbreviations used to identify each protein correspond to Brookhaven protein data bank codes.[23] (B) The distance distribution function for aromatic side chain centroid separation (<10 Å). Each value of the distribution function was normalized for sample size by dividing by $4\pi r^2$. (C) The interplanar angle distribution function for all aromatic pairs separated by less than 6.5 A. The expected distribution, given by sine of the interplanar angle (sin (D)), is depicted with the symbol "o". The mean interplanar angle ($\langle D \rangle$) with its expected value of 57° and $\chi^2/8$ are also given. (D) A histogram of the calculated potential energy of interaction for all aromatic pairs separated by less than 6.5 Å.

is colinear with the x axis (see Figure 1A). The angle between the two ring planes and the position in polar coordinates (r, θ, ϕ) of the interacting ring centroid were calculated for every pair of aromatic side chains less than 10 Å from center to center in the 33 protein structures.

Aromatic pairs meeting criteria described below were retained and their interaction geometries were analyzed by the following procedure: The data base of retained pairs was subdivided into interaction classes by the polar coordinate θ and further subdivided by the interplanar angle. The expected distribution of interplanar angles for each interaction geometry subclass was calculated and illustrated by points superposed on the frequency histograms. This expected distribution is a function of both the sine of the interplanar angle and the sine of the angle θ and describes random packing of planar molecules in space. Mean interplanar angle and (χ^2), the goodness-of-fit between observed and expected distributions, were calculated for each interaction geometry subclass. In addition, the goodness-of-fit between the observed distribution and the appropriately normalized function sin (interplanar angle) was calculated.

Nonbonded Interaction Energy Calculations. The nonbonded interaction energy for each pair of retained aromatic side chains was calculated with use of an approach formulated from ab initio quantum mechanical calculations of dibenzene.[7] In addition, the potential energy surface for dibenzene as a function of ring separation geometry and interplanar angle was calculated.

The nonbonded potential energy model for benzene developed by Karlström et al.[7] and given by

$$E = \sum_{jk} A_{jk} r_{jk}^{-1} + B_{jk} r_{jk}^{-4} + C_{jk} r_{jk}^{-6} + D_{jk} r_{jk}^{-9} + E_{jk} r_{jk}^{-12}$$

was chosen on the strength of its specific development for dibenzene, including reproduction of the existence of a dipole moment and an accurate estimate of the experimental quadrupole moment.[11,12] The model was constructed by fitting the above analytic potential function to the results of ab initio calculations of dibenzene in 72 different relative orientations, some highly symmetric and others random. Each interacting atom pair j,k in the two nearby phenyl rings, separated by a distance r_{jk}, is described by the parameters A_{jk}, B_{jk}, C_{jk}, D_{jk}, and E_{jk}, which depend on atom type j and k. Some of the terms in the power-series expansion have established physical meanings; r^{-1} is the coulombic term describing the interaction between partial charges; r^{-6} and r^{-12}, the 6/12 potential terms, describe van der Waals' interactions. The calculation compares the interaction potential energies of a nearby pair of aromatic side chains and the same residues infinitely far apart.

The power-series model of Karström et al.[7] provides superior agreement with both experimental data and ab initio dibenzene calculations to the Evans and Watts empirical benzene–benzene potential[12,13] and represents one of the few computationally feasible approaches to evalu-

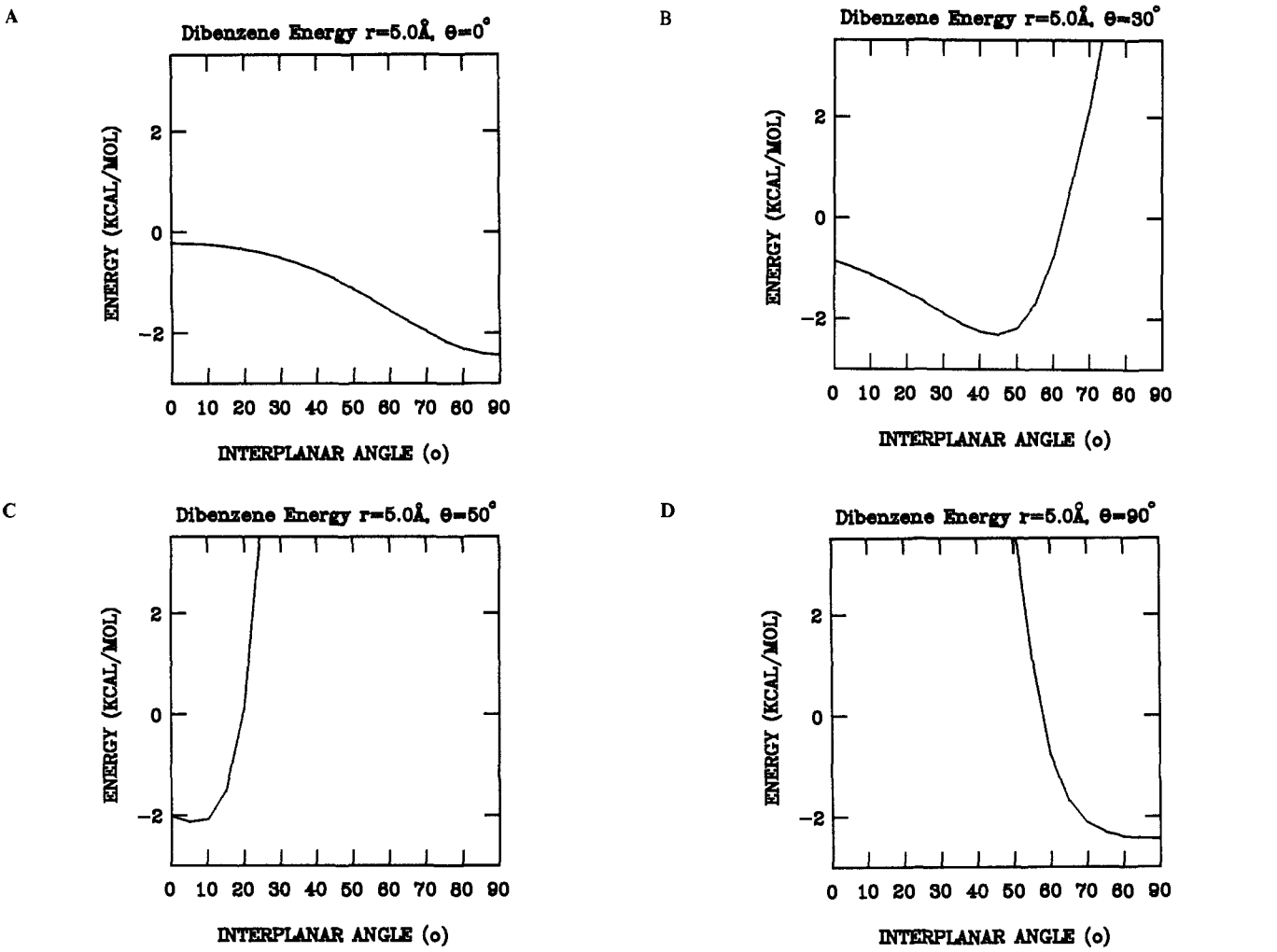

Figure 2. The potential energy surface for two interacting benzene molecules separated by r = 5.0 Å displayed as a function of the polar coordinate angle θ and the angle between the two planar molecules (**D**).

ation of the entire dibenzene potential energy surface. In addition, the potential function has been extensively tested against other experimental data.[14] Approximate ab initio calculations of dibenzene with use of the partial retention of diatomic differential overlap method[15] did not reproduce either the experimental observations or the results of Karlström et al.[7] (data not shown).

Results

Geometric Analysis of Aromatic Pairs in Proteins. The frequency distribution of aromatic side chain centroid separations, illustrated in Figure 1B, is sharply peaked near 5.5 Å. A total of 580 pairs of aromatic side chains were found with centroid separations of 10 Å or less. Of this group, 225 pairs had centroid separations of between 3.4 and 6.5 Å and were retained for further analysis. The expected number of pairs falling within this range of centroid separations can be calculated from volume considerations and is 139. Below 3.4 Å centroid separation aromatic pairs, which would made unfavorable van der Waals' contacts, were not observed. Beyond about 6.5 Å separation, the observed distribution of aromatic pairs is nearly constant and reflects the spatial distribution of all amino acids in globular proteins.[3,9]

Figure 1C shows the observed frequency distribution of interplanar angles for the 225 retained aromatic pairs and the expected angular distribution assuming random orientation of planar side chains. The observed distribution does not differ significantly from the exptected distribution ($\chi^2/8 = 0.39$), and the probability that a random set of data points would yield a value of χ^2 as large or larger than the obtained value is 0.92.

Energetic Analysis of Aromatic Pairs in Proteins. The histogram of calculated interaction energies of aromatic pairs in proteins is illustrated in Figure 1D. Eighty-four percent of the aromatic side chain pairs make energetically favorable interactions, and the distribution is peaked about an enthalpic contribution of approximately −1.2 kcal/mol. Of the remaining 16% of the cases, 8% are somewhat enthalpically unfavorable and the other 8% have markedly unfavorable enthalpies. Some of these enthalpically disfavored interactions clearly result from unfavorable van der Waals' contacts that probably reflect incomplete refinement of portions of the protein's structure. In addition, both inaccuracies of the energetic model and locally unfavorable side chain packing that allows commensurately favorable packing of side chains elsewhere in the protein could explain calculated repulsive potential energies.

Dibenzene Potential Energy Surface. Representative portions of the dibenzene interaction energy surface are displayed in Figures 2, 3, and 4 for values of r = 5.0, 5.5, and 6.0 Å, respectively. The ϕ dependence of the potential energy function is small, except where the two benzene rings are in van der Waals' contact, and is, of course, invariant to 6-fold rotation about the z axis of the reference coordinate system (data not shown).

The dependence of the potential energy on θ and interplanar angle is not simple. For values of θ between 0 and 22.5° where the two ring centroids lie near the 6-fold symmetry axis of the

(12) Evans, D. J.; Watts, R. O. *Mol. Phys.* **1975**, *29*, 777.
(13) Evans, D. J.; Watts, R. O. *Mol. Phys.* **1976**, *31*, 83.
(14) Linse, P. *J. Am. Chem. Soc.* **1984**, *106*, 5425.
(15) Halgren, T. A.; Lipscomb, W. N. *J. Chem. Phys.* **1973**, *58*, 1569.

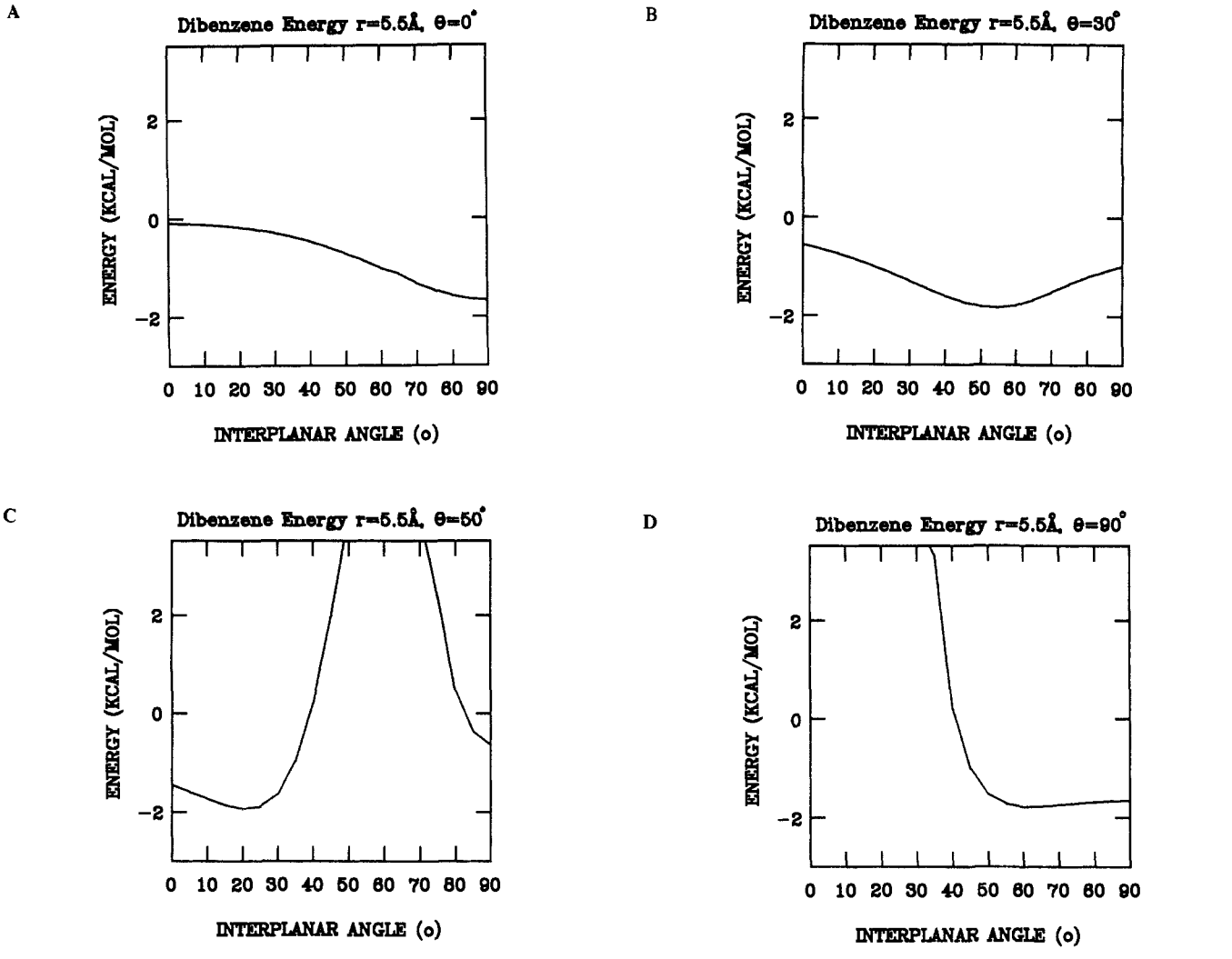

Figure 3. The potential energy surface for two interacting benzene molecules separated by r = 5.5 Å displayed as a function of the polar coordinate angle θ and the angle between the two planar molecules (D).

reference ring, interplanar angles approaching 90°, the "T-stacked" arrangement, are enthalpically favorable, with the potential well minima at 90° (see Figures 2A, 3A, and 4A). As θ increases to between 22.5 and 45° the potential energy minima occur at values of interplanar angle between 45 and 60° (see Figures 2B, 3B, and 4B). For values of θ between 45 and 67.5°, the potential energy minima occur at interplanar angles between 5 and 35°, and at 90° (see Figures 2C, 3C, and 4C). Finally, when the two ring centroids lie in or near the plane of the reference ring ($\theta \simeq 90°$) the potential energy minima occur at interplanar angles between 45 and 90° (see Figures 2D, 3D, and 4D).

The geometric arangements of dibenzene corresponding to the potential energy minima identified in parts A–D in Figure 3 are displayed as van der Waals' stereodrawings in Figure 5. These drawings indicate that within each angular range enthalpically optimal interactions occur when the $\delta(+)$ H atoms at the edge of one ring approach the $\delta(-)$ π-electron cloud of the other benzene ring. The global potential energy minimum, $E \simeq -2.4$ kcal/mol, occurs when the benzene planes are perpendicular to one another with their centroids coincident with the 6-fold symmetry axis of one ring and separated by 5.0 Å, the "T-stacked" configuration. As documented in Figures 2, 3, 4, and 5, the values of θ and interplanar angle corresponding to the potential energy minimum for each value of r are not constant; their variation allows access of the $\delta(+)$ hydrogen atoms of one aromatic group to the $\delta(-)$ π-electron cloud of the other. A local potential energy minimum, $E \simeq -1.8$ kcal/mol, was found for two horizontally stacked benzene molecules with a vertical separation of 3.3 Å and with their centroids separated by 4.4 Å in the horizontal [(5.5 Å, 53°, 0°), in the polar coordinate system illustrated in Figure 1A]. This minimum was predicted by Gould et al.[1] from their analysis of phenylalanine single-crystal structures.

Further Geometric Analysis of Aromatic Pairs in Proteins. The observed distribution of interaction geometries is not comparable to that expected if the planar aromatic side chains were packed in the protein's interior in a random fashion. Instead, the observed frequency distributions of different interaction geometries are a function of the ring–ring overlap and are well corelated with the shape of the energy surface depicted in Figures 2, 3, and 4 and the interaction geometries shown in Figure 5.

The case of two phenyl rings with $0 < \theta < 22.5°$, illustrated in Figure 6A, is preferred over $\theta > 45°$ and occurs with 20% more than the predicted frequency ($N_{obsd}/N_{predicted} = 20/17.1 = 1.2$). Within this subgroup interplanar angles (D) between 50 and 90° are markedly preferred; the mean interplanar angle ($\langle D \rangle$) is 68°, which should be compared to the predicted value given by $\int_0^{\pi/2} D \sin(D)\, dD \simeq 57°$. $\chi^2/8$ between the observed and expected distributions equals 1.30, and $\chi^2/8$ between the observed distribution and normalized sine of the interplanar angle ($\sin(D)$) equals 1.02. Therefore, there are statistically significant differences between the observed and expected distributions illustrated in Figure 6A. These differences are well correlated with the cal-

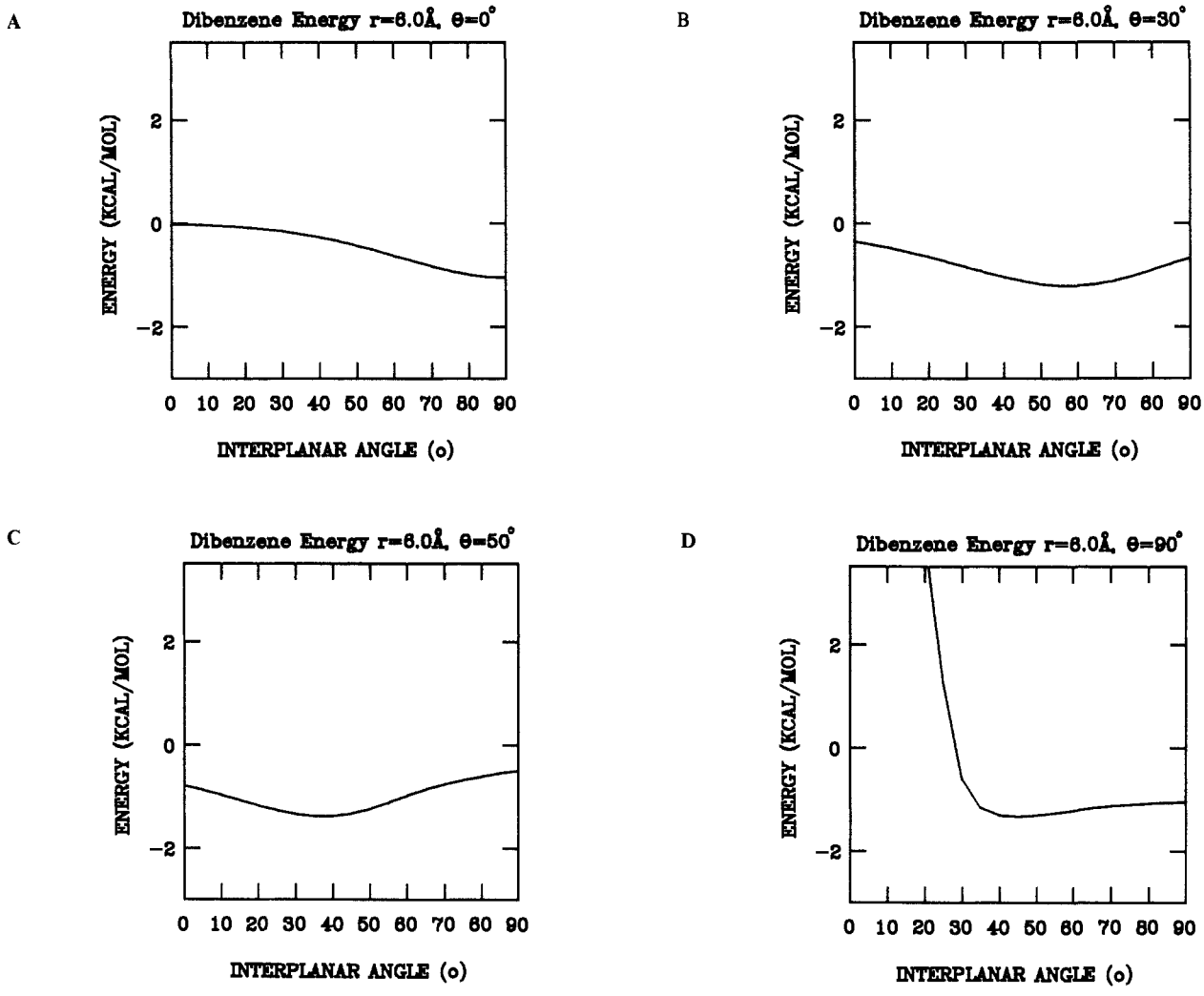

Figure 4. The potential energy surface for two interacting benzene molecules separated by r = 6.0 Å displayed as a function of the polar coordinate angle θ and the angle between the two planar molecules (**D**).

culated potential energy curves shown in Figures 2A, 3A and 4A.

The subclass of aromatic pairs with $22.5 < \theta < 45°$, illustrated in Figure 6B, was detected with about 20% more than the expected frequency ($N_{obsd}/N_{predicted}$ = 57/48.8 = 1.2). The largest deviation from the expected distribution given by sin (D) occurs at interplanar angles between 50 and 70°. $\langle D \rangle$ = 57° with a predicted value of 57°. $\chi^2/8$ between the observed and expected distributions equals 1.44, and $\chi^2/8$ between the observed distribution and normalized sin (D) equals 0.71. Again, there are statistically significant differences between the observed and expected distributions illustrated in Figure 6B, which are well correlated with the potential energy curves displayed in Figures 2B, 3B, and 4B.

The case of $45 < \theta < 67.5°$, shown in Figure 6C, was detected with almost the expected frequency ($N_{obsd}/N_{predicted}$ = 76/73.0 = 1.05), and within this subgroup interplanar angles between 0 and 40° and at 90° are preferred. $\langle D \rangle$ = 52° with a predicted value of 57°. $\chi^2/8$ between the observed and expected distributions equals 1.66, and $\chi^2/8$ between the observed distribution and normalized sin (D) equals 1.04. Therefore, there are statistically significant differences between the observed and expected distributions illustrated in Figure 6C, and these differences are well correlated with the calculated potential energy curve shown in Figures 2C, 3C, and 4C.

Finally, the case of $67.5 < \theta < 90°$, shown in Figure 6D, is only detected with an observed frequency of 84% of the expected value ($N_{obsd}/N_{predicted}$ = 72/86.1 = 0.84). Within this subgroup the interplanar angles between 40 and 90° are preferred. $\langle D \rangle$ = 62° with a predicted value of 57°. $\chi^2/8$ between the observed and expected distributions equals 1.29, and $\chi^2/8$ between the observed distribution and normalized sin (D) equals 1.16. Again, there are statistically significant differences between the observed and expected distributions illustrated in Figure 6D. This subclass of interaction geometries is disfavored, but within this group the largest deviations from the expected distribution occur for interplanar angles between 50 and 80°, which correlate well with the potential energy function shown in Figures 2D, 3D, and 4D.

When aromatic pairs are arranged in the "T-stacked" state the two cases θ = 0 and 90° corresponding to the global energy minimum are identical and represent the most frequently observed interaction geometry subgroup in proteins (number of pairs = 17). Unlike the phenylalanine single-crystal structures surveyed by Gould et al.,[1] the horizontally stacked configuration, analogous to the stacking of bases in DNA, is only rarely observed in proteins.

Summary. These data indicate that aromatic side chains in proteins preferentially form pairs with centroid separations between 3.4 and about 6.5 Å. The majority of aromatic pairs detected in the 33 surveyed protein structures make enthalpically favorable nonbonded interactions. The observed frequency distributions of both aromatic-pair spatial separation and interplanar angle differ significantly from the distributions expected if random orientations alone determined interaction geometry. In fact, the documented deviations from "random" reflect a statistically significant pref-

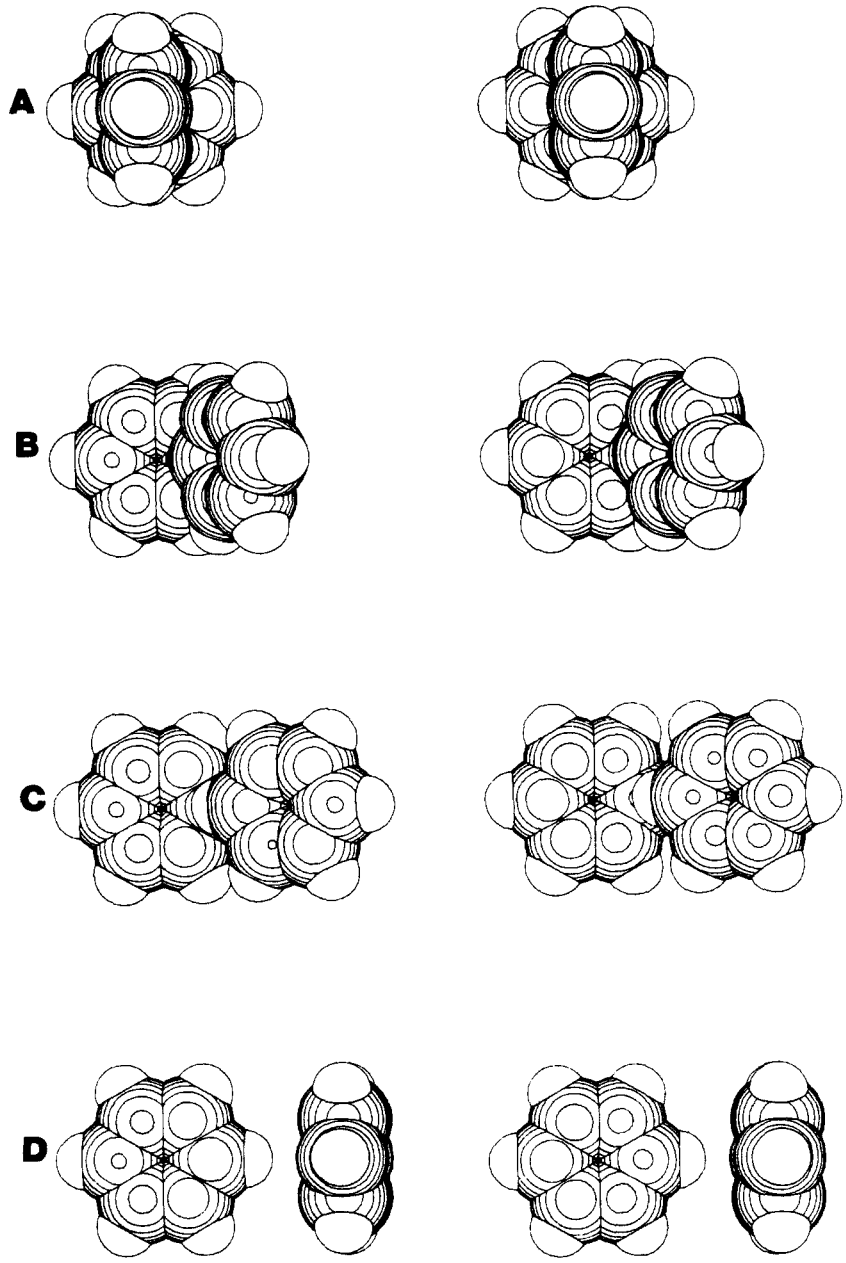

Figure 5. van der Waals' stereo drawings of interacting benzene rings positioned in each of the enthalpically optimal geometric arrangements for r = 5.5 Å identified as potential energy minima in parts A–D of Figure 3. (A) $\theta = 0°$, interplanar angle = 90°; (B) $\theta = 30°$, interplanar angle = 55°; (C) $\theta = 50°$, interplanar angle = 20°; (D) $\theta = 90°$, interplanar angle = 90°.

erence for energetically favorable geometries determined from the potential energy surface of dibenzene.

Discussion

We suggest that packing of aromatic side chains in the hydrophobic core of a protein is determined by at least 2 requirements: (1) the need to exclude water molecules, and (2) the formation of a large number of ethalpically favorable, weakly polar interactions resulting from the large quadrupole moment of aromatic side chains. Although each interaction between pairs of aromatic side chains is only capable of contributing between −1 and −2 kcal/mol to protein structure stability, there are on average 7 such interactions per protein, and their total enthalpic contribution is not insubstantial. Moreover, energetically favorable edge-to-face interactions between aromatic side chains have also been observed in oligopeptides bearing two or more aromatic residues where they play an important role in stabilizing biologically active conformations. Crystal structures of 4 bisphenyl oligopeptides and peptide analogues, all model therapeutic agents for the treatment of sickle cell disease, document that their compact, amphipathic conformations are maintained by edge-to-face interactions between phenyl rings.[16] Proton magnetic resonance studies of somatostatin also demonstrate an edge-to-face interaction between the side chains of phenylalanine residues 6

(16) Burley, S. K.; Wang, A. H.-J.; Votano, J. R.; Rich, A. *Biochemistry*, submitted.
(17) Arison, B. H.; Hirschmann, R.; Paleveda, W. J.; Brady, S. F.; Veber, D. F. *Biochem. Biophys. Res. Commun.* **1981**, *100*, 1148.
(18) Giammona, A.; Field, M.; Smith, J.; Karplus, M., work in progress.
(19) Weiner, S. J.; Kollman, P. A.; Nguyen, D. T.; Case, D. A., manuscript in preparation.
(20) Frauenfelder, H.; Hartmann, H.; Karplus, M.; Kuntz, I. D., Jr.; Kuriyan, J.; Parak, F.; Petsko, G. A.; Ringe, D.; Tilton, R. F. T., Jr.; Connolly, M.; Max, N. *Biochemistry*, in press.
(21) Tsernoglou, D.; Petsko, G. A. *Proc. Natl. Acad. Sci. U.S.A.* **1977**, *74*, 971.
(22) Gilbert, W.; Petsko, G. A. *Biochemistry*, manuscript in preparation.

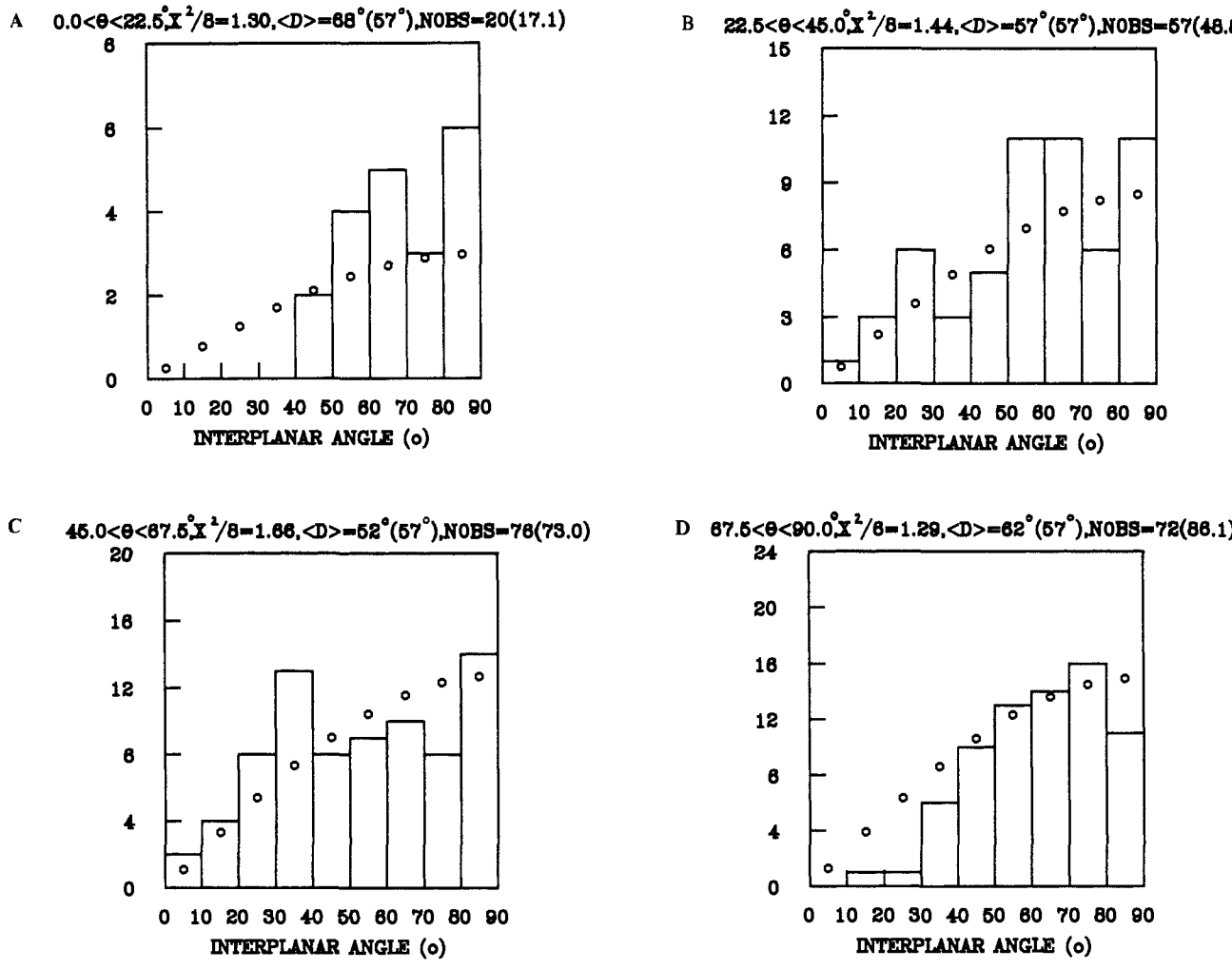

Figure 6. The observed distribution of interplanar angles between the 225 interacting pairs of aromatic side chains displayed as a function of polar coordinate angle θ. Each panel A, B, C, and D is comparable to the same panel in Figures 2, 3, 4, and 5. The expected interplanar angle distribution, given by sin (D), is illustrated by the symbol "o" on each panel, with the corresponding values of the observed and expected number of observations in each chosen range of θ and the value of $\chi^2/8$ describing the goodness of fit between the observed and expected distributions. The mean observed interplanar angle ($\langle D \rangle$) is also given in each panel, with its expected value of 57° in parentheses.

and 11 that creates a pseudo-bicyclic molecule and is essential for biological activity.[17]

Conclusion

We have documented the existence of an enthalpically favorable, weakly polar interaction between aromatic side chains in proteins. Similar weak but numerous nonbonded interactions involving other chemical groups in proteins have also been documented by surveying the large data base of crystal structures,[1,2,4] and the list is by no means complete. We conclude that theoretical studies of protein physics should include these newly described interactions, and recent development of "all-atom" force fields for molecular mechanics calculations reflects this need.[18,19]

Acknowledgment. We thank Drs. J. Singh and J. M. Thornton for early communication of their studies of phenylalanine dimers in proteins and Dr. R. F. Tilton, Jr., for his critical comments.

(23) Bernstein, F. C.; Koetzle, T. F.; Williams, G. J. B.; Meyer, E. F., Jr.; Brice, M. D.; Rodgers, J. R.; Kennard, O.; Shimanouchi, T.; Tasumi, M. *J. Mol. Biol.* **1977**, *112*, 535.